Valentin Plenk (ed.)

Proceedings of the 1st International Research Colloquium

Hof

2015

Hofer Akademische Schriften

Prof. Dr. Valentin Plenk (ed.)

Proceedings of the 1st International Research Colloquium

Hof, 2015

The Authors
Corinna Anzer
Roland Krause
Sabine Olbrich
Prof. Dr. Brando Okolo
Annette Wimmer

Verlag

Hochschule für Angewandte Wissenschaften Hof, Alfons-Goppel-Platz 1, 95028 Hof/Saale

ISBN 978-3-935565-37-0

Table of contents

Preface by Prof. Dr. Dr. h.c. Jürgen Lehmann, President of Hof University

Internationalization is an integral part of science and research. In accordance with its profile and mission, Hof University has been advancing the internationalization of teaching and research with numerous offers and events, such as the International Teaching Week.

During the second International Teaching Week (June 8th to 12th, 2015), we welcomed guest lecturers from five countries at Hof University. The Teaching Week also included our first International Research Colloquium, which took place on June 8th at the Institute for Materials Science (ifm). About 30 students and researchers from Hof University and abroad participated in the colloquium, which provided a platform for presenting research activities and exchanging ideas in the field of materials science.

We have chosen to make publicly available all papers presented at the colloquium by publishing them together in a single volume.

We would like to warmly thank the following people who have made this volume possible: Prof. Dr. Valentin Plenk, Dr. Wolfgang Bauch, Prof. Dr. Brando Okolo, Corinna Anzer, Sabine Olbrich, Annette Wimmer and Roland Krause.

Energy Efficient Textile Heating System based on Carbon Nanotubes (CNTs)

M. Eng. Corinna Anzer, Prof. Dr. Frank Ficker, Dr.-Ing. Wolfgang Althaus*, Dipl. Chem. Birgit Müller, Dipl. Ing. (FH) Alexandra Luft
Institute for Material Science – University of Applied Sciences Hof
* thermofer GmbH & Co. KG, Köln
corinna.anzer@hof-university.de

Keywords: textile heating system, panel heating system, carbon nanotubes

Abstract

Due to the rising energy prices energy efficient heating systems become more and more attractive. Next to the energy consumption the comfort is a very important criterion. Conditioned by these requirements the number of panel heating systems will increase in the future. To comply with the customer request infrared (IR) radiation is suitable, because of the reduced dust emergence and noise emission in comparison to standard heaters. Infrared heating systems are beneficial to health and create a “feel-good” climate. Based on these aspects a ZIM-supported project was initiated to develop an innovative textile heating system using carbon nanotubes (CNT), which emit infrared radiation.

Initial position and motivation

Available radiant heating systems are currently classified into different groups. Customary in the market are water-based underfloor systems, textile heaters with incorporated electrical conductive fibers like copper or carbon, heating systems using cables as well as polymeric heating technologies. In comparison to these products the aim of the project “Energy Efficient Textile Heating System based on Carbon Nanotubes” (KF2429507HF2), which was supported by the federal ministry for economic affairs and energy, was to develop a heating textile for the thermal activation of cement structures. Benefits of the technology are the design of an open textile structure to achieve an excellent embedding performance without a negative influence on the cement properties like delamination or a strength decrease. The copper electrodes are integrated into the heating element and not bonded. This design ensures a good connection between the heating element and the electrodes and as consequence a reduction of security risks caused by a delamination. Figure [1] shows the homogeneous heating in comparison to a floor heating system using cables with hot cables and a cold surrounding resulting in high temperature gradients generating high thermal stresses.

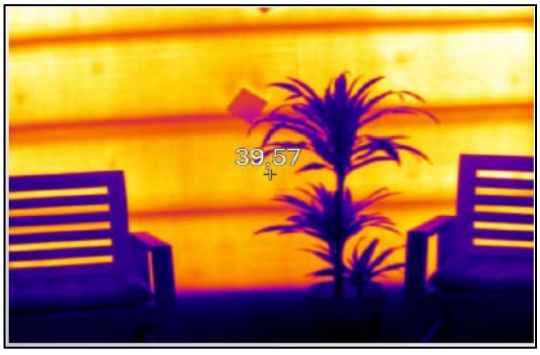

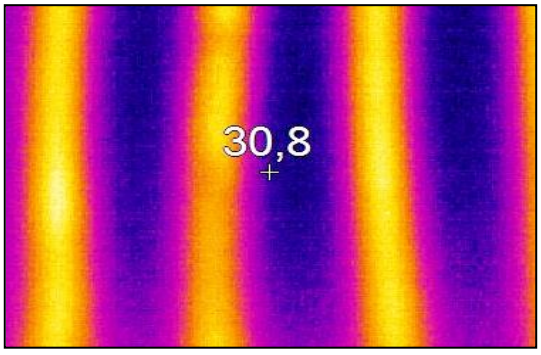

Figure [1]: Thermographic picture of the CNT-heating system (left) and a cable-based heating technology (right)

In summary the aim of the project was the development of an alkali-resistant textile heating system with an open, flexible and resistant mesh structure, an even heat distribution and a high energy efficiency level, which is combinable with renewable energy like photovoltaic or small wind turbines and which is insertable in cement without a negative influence on the composite properties.

Function principle and development steps

The basic construction of the textile heating system is a glass fiber leno weave fabric with two integrated copper electrodes on both sides of the element, which are contacted with crimps, and with an electrical conductive area between (figure [2]). Therefore, a CNT-coating was applied on the woven structure. Carbon Nanotubes are allotropes of carbon with a cylindrical nanostructure and a high electrical conductivity. Due to the application of voltage carbon nanotubes emit infrared radiation and heat up the surrounding.

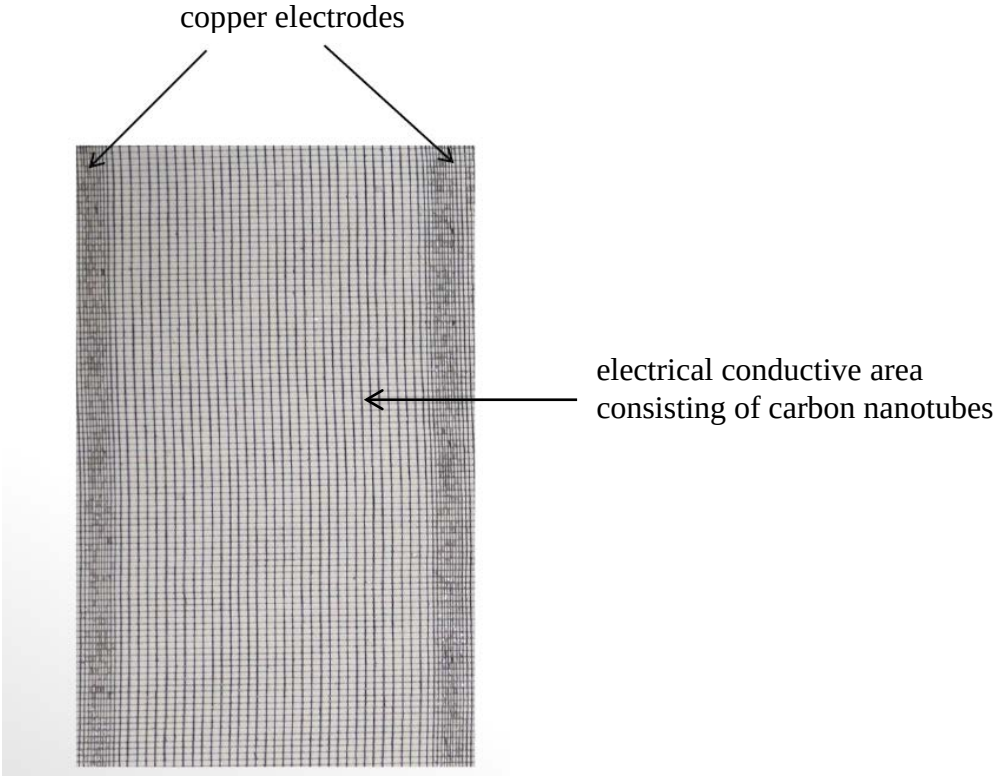

Figure [2]: Function principle of the CNT-heating textile

In the first development step the textile structure of the panel heating system was designed. Therefore trials with a plain and a leno weave structure, with copper insertion in warp and weft direction as well as the use of different types of glass yarns like sliver, texturized rovings and glass silk was carried out. The best results regarding the reduction of the risk of yarn displacement in combination with an open mesh structure were achieved with the leno weave fabric. Due to this open mesh structure the required embedding performance in cement can be guaranteed. Table [1] shows the characteristics of the developed woven textiles.

Table [1]: Woven fabric characteristics

textile structure	copper insertion	cross section copper	mesh size woven fabric	grammage woven fabric
1	weft thread	0,4 mm	5 x 8 mm	130 g/m^2
2	weft thread	0,2 mm	5 x 8 mm	130 g/m^2
3	warp thread	0,4 mm	7 x 10 mm	95 g/m^2

The cross section of the copper depends on the current applied. A higher current results in a higher necessary copper cross section. The integration of copper as warp thread has benefits regarding the tailoring, because an individual length of the heating element can be achieved. Figure [3] shows the basic leno weave structure as well as the CNT-coating.

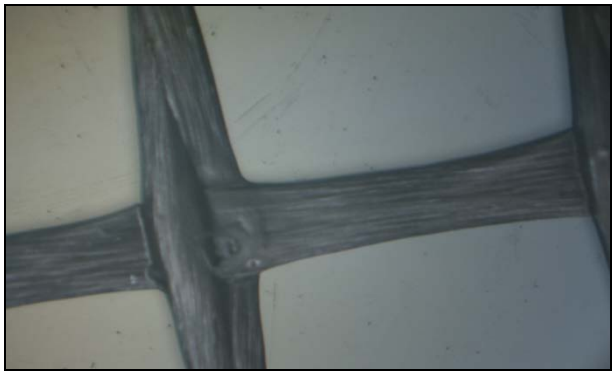

Figure [3]: Basic leno weave structure and CNT-coated fabric

The selection of the glass fibers was based on the CNT-adsorption of the textile after the coating process. The results show a high CNT-adsorption using sliver and texturized yarns with an open appearance and projecting fibers, which is causing a closing of the meshes. Unlike glass silk enables a homogeneous coating without mesh closing.

The coating of the leno weave with a water-based CNT-dispersion was carried out by the foulard-technology. After the impregnation in a dipping bath the surplus coating was squeezed. Following the textile element passes the heat treatment and dryer to evaporate the water of the dispersion. As results of different trial runs an evenly coating without mesh closing is possible. The resistance of the heating element can be defined adjusted by the grammage of the CNT-layer and the number of layers. The required electrical resistance was achieved with a single CNT-layer with an area weight of 10 g/m^2.

The performed tests on the heating system also offered a spalling of the CNT-layer during the handling. This fact is very critical because of the CNT-dust emergence, which can cause health issues, as well as because of the change of resistance. Due to these requirements a protective layer was applied to fix the carbon nanotubes. The top coat has to ensure an alkali-resistance and waterproofness in dependence on the application in cement structures. An electrical insulation is not necessary, because the system is operated with safety extra-low voltage (SELV). Within the investigations a two-layer styrol butadien rubber (SBR) coating shows the best performance relating to the foulard coating process and the specification. SBR offers an evenly coating

without a mesh closing and does not cause a change of the resistance of the heating system in comparison to other coating dispersions used. In these cases the reason for the increasing resistance after the top layer application is an entry of the dispersion into the CNT-layer, which results in a change of the conductive circuit. The foulard coating process for CNT- and protective layer is shown in figure [4].

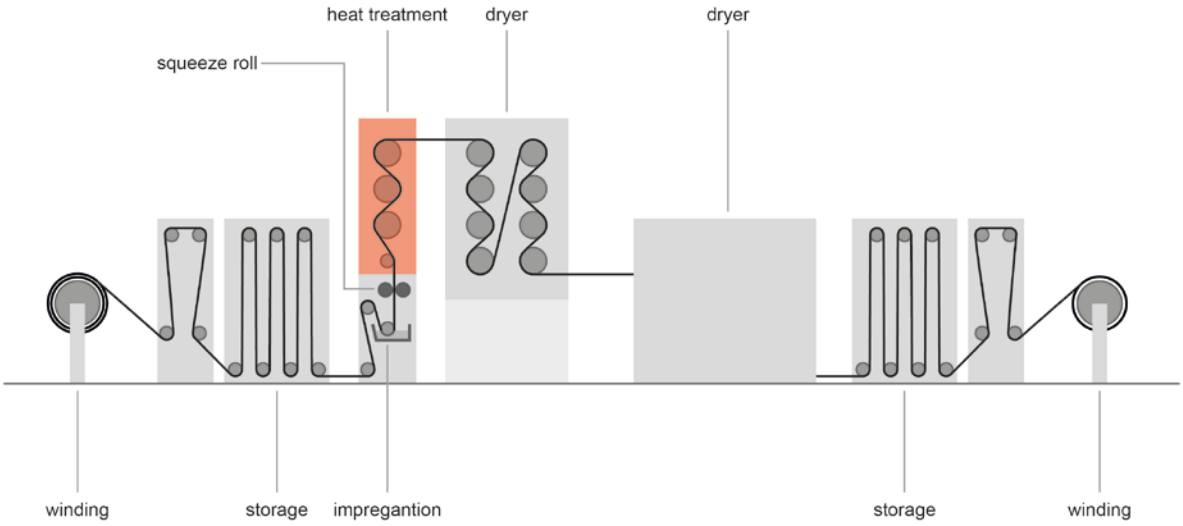

Figure [4]: Foulard-coating process

For the analysis of the life time properties the heating system was embedded in a cement block and heated. As one result the embedding in fine and coarse cement without causing damages of the heating film is possible. Next to this the tensile strength of cement with the integrated mesh was equal to the reference value of pure cement. The life time testing is still in progress to analyze the heating performance as well as the alkali-resistance under operating conditions. During the production of the heating element the resistance was constantly measured and allows the process control.

Summary

The design of an energy efficient textile heating system with an excellent embedding performance without a negative influence on the cement properties was implemented within the development project. Due to the continuous production methods of leno weaving and foulard coating a commercial product with a wide range of applications in historical buildings and for the restoration of old buildings was developed. The low installation and servicing costs, the energy efficiency as well as the invisibility of the system support the use. A performed testing shows that the specific energy consumption of the heating textile in a not insulated room is three times lower in comparison to a not rehabilitated house with standard heaters. Further development steps should target the design of heating system for 230 V applications including the necessary electrical insulation layer for large-scale heating applications.

The project was supported by the federal ministry for economic affairs and energy (KF2429507HF2) and carried out in cooperation with thermofer GmbH & Co. KG and Elektro-Bergmoser GmbH & Co. KG.

Investigation of energy demand and waste heat occurrence during the extrusion process of tubular profiles

Roland Krause [1,a] and Herbert Reichel [1,b]

[1]Hochschule Hof, Institut für Materialwissenschaften,
Alfons-Goppel-Platz 1, 95028 Hof/Saale

[a]roland.krause@hof-university.de, [b]herbert.reichel@hof-university.de

Abstract

Extrusion is a fundamental procedure of polymer processing and is used to produce tubular profiles, foils, cable coatings, etc. Rising energy prices increase the pressure for extruder manufacturers and operators to cut costs. Nowadays, extruder manufacturers are forced to develop more energy-efficient extruders. One possibility to reach that goal, is to reuse the occurring waste heat during the extrusion process. Operators could use the waste heat within their own company to reduce their primary energy costs. Therefore, determination of energy flows of small to medium-sized extrusion lines was necessary. The two major sources of waste heat during the extrusion of tubular profiles are the vacuum chamber and the barrel cooling. The process energy demand has been monitored under various processing conditions for two different single grooved barrel extruders (SGBE) and two different tubes. Additionally the energy consumption of the main consumers has been monitored. The energy monitoring results show that the waste heat within the vacuum chamber of SGBE 9 sums up to an energy amount which can and should be used. Furthermore the quantity of waste heat depends highly on the geometry of processed tubular profiles. The bigger tubular profile which translated to a higher output rate had a much higher waste heat than smaller tubes. The specific energy consumption of extruder type SGBE 5 reduced with increasing screw speed whereas the opposite was monitored for extruder type SGBE 9.

1. Introduction

1.1. Determination of waste heat as part of energy flows

Extruders are primarily supplied with electrical energy which is converted into mechanical and thermal energy. Mainly the mechanical energy is used to drive a rotating screw which is connected to a motor. Thermal energy is fed into the process via barrel heaters. Waste heat occurs at multiple points of an extrusion line. The main waste heat sources are the barrel, grooved barrel and transmission unit and cooling devices which consist of a vacuum chamber and various cooling chambers. Usually, the cooling devices are the components which take a high amount heat out of the polymer and collect this by water. Futhermore, heat is absorbed by air during the product stabilization. On the other hand waste heat occurs on the surfaces of the barrel and the product by radiation. The amount of generated waste heat in the extrusion process is not well documented. Strauch [1] mentioned that over 50% of the inserted energy is absorbed by the cooling water whereas radiation and free convection have a major impact with regard to energy losses. Drury [2] stated that the reusage of waste heat has little potential because it is primarily bound in water or air. Furthermore, Drury argued that almost half of the supplied energy is lost via

drive and transmissions, radiation, convection, conduction etc. Bastian [3] proposed that the waste heat could be used to preheat the input material which gains a higher enthalpy level and leads to a lower melting capability.

1.2. Determination of energy flows of the main consumers

Usually, the main energy consumers of an extrusion line are the drive motor, barrel heaters, die heaters, melt pump and auxiliary units like circulating and vacuum pumps. Figure 1 shows a typical energy flow diagram for an extruder. If you compare the energy consumption of all electrical consumers the drive motor consumes by far the most electrical energy. Heur and Verheijen [4] stated that most of the supplied electrical energy is used by the motors, heating and cooling devices as well as compressors. Furthermore they stated that the energy consumption depends on the used polymer, configured process parameters and plants. Barlow [5] reported that the motors of an extrusion plant consume 33% of the supplied electrical energy. Brown [6], Kelly [7], Cantor [8] and Abeykoon [9] mentioned that with increasing screw speed the extruder specific energy consumption (SEC) is decreasing.

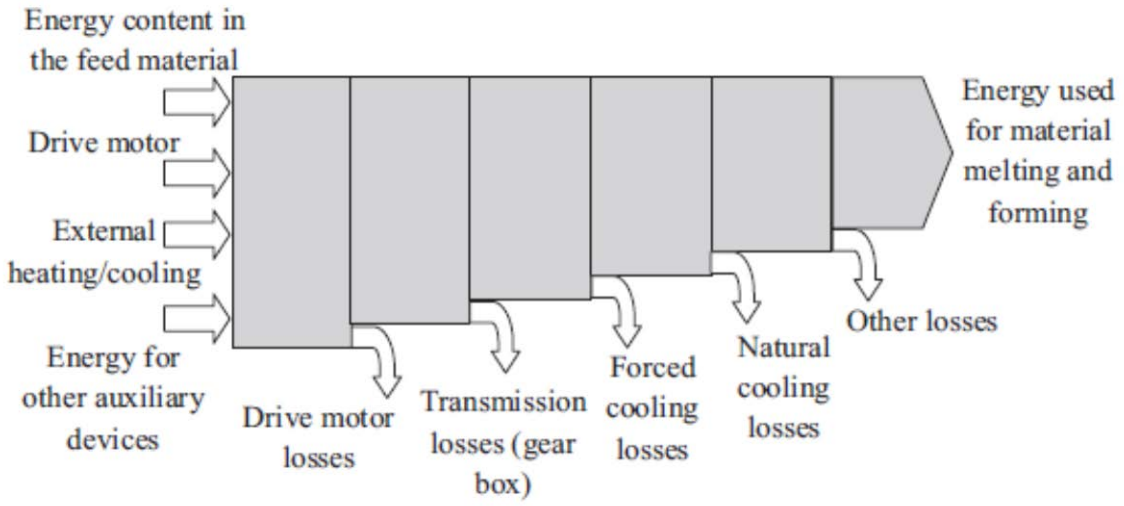

Fig. 1. Flow diagram for an extruder [9]

2. Equipment and procedure

2.1. Waste heat monitoring in the vacuum chamber

The waste heat monitoring experiments were carried out on a 90mm diameter (D) single grooved barrel extruder type SGBE 9 (Weber Maschinenfabrik GmbH) with 310 kW installed power. The extruder barrel has five separate temperature zones of 5,4 kW each with five and additional die heaters in the 1,2-5,5 kW range. The object of the waste heat monitoring was the vacuum chamber that is divided into two chambers which are completely separated from each other. Within the chamber water is used as a coolant. In each chamber heat absorbed in water flows through a heat exchanger which is fed with water as the second fluid. The water temperatures in the two chambers are set at around 45 °C for the first chamber and at around 25 °C for the second chamber whereas the second fluid temperature is set at 20 °C. The volume flow as well as the flow temperature and return flow temperature were measured using an

Allmess CF ECHO II ultrasound heat meter. To transfer the data from the ultrasound heat meter to the PC a RELAY RS232C MR006FA data converter was used. The data was saved every minute using the Windows Scheduler.

2.2. Extruder energy monitoring of the main consumers

The determination of energy flows was performed at two medium-sized extrusion lines. One of the two extruders was already mentioned in the previous abstract, the other one is a 50mm diameter single grooved barrel extruder type SGBE 5 (Weber Maschinenfabrik GmbH) with 117 kW installed power. The extruder barrel has four separate temperature zones of 2,5 kW and six die heaters of 0,35-2,2 kW. The current measurement includes the overall power consumption and the main power consumers extruder drive with frequency converter, barrel heaters, die heaters and melt pump. The power consumption was recorded using an Arnoux Chauvin Power & Energy Logger 103.

2.3. Material and experimental conditions

Experimental trials were carried out on a polypropylene homopolymer with density: 0.910 g/cm^3 and melt flow rate (MFR): 2.1 g/10 min @ 230 °C, 2.16 kg for all experiments. Two tubular profiles (P1) and (P2) with different inner-/external-diameters were part of the waste heat and energy monitoring. The extruder barrel temperature settings were set at 200°C. The haul-off speed was set at 0,7 m/min and 0,8 m/min for P1 as well as 0,71 m/min and 1,0 m/min for P2.

3. Results and discussion

3.1. Experimentally measured extruder waste heat in the vacuum chamber

Initially, experimentally measured signals with the ultrasound heat meter of the vacuum chamber were studied. The other waste heat sources like grooved barrel and transmission unit could be neglected due to its low cooling capacity. The cooling chambers have not been part of the energy monitoring because of the low coolant temperature. The average values of total cooling power (P_C), volume flow rate per hour ($\dot{V}_{CW}$), difference between water flow temperature and return flow temperature (ΔT), return flow temperature (T_R), haul-off speed (v_{HO}) and material output ($\dot{m}$) over the whole measuring period of the tubular profiles P1 and P2 are shown in Table 1. As expected, the total cooling power of the tubular profile P1 was significantly higher in comparison to tube P2. This can be explained by the higher output rate of P1. The power values of 22 kW (P1) and 14,5 kW (P2) collected by the coolant show that for both tubular profiles a waste heat utilization is useful. Additionally it can be stated that in chamber 1 most of the power was transferred to the water. Previous work reported by Bastian [3] mentioned that waste heat could be used for preheating the input material.

Table 1
Test parameters of the waste heat monitoring in the vacuum chamber

Product	Vacuum Chamber	T_R [°C]	ΔT [K]	$\dot{V}_{CW}$ [m^3/h]	P_C [kW]	v_{HO} [m/min]	$\dot{m}$ [kg/h]
P1	C1	28,6	1,2	11,5	15,6	0,65	163,9
	C2	45,4	0,6	8,6	6,4		
P2	C1	28,6	1,1	11,1	11,4	1,0	112,7
	C2	45,3	0,3	8,4	3,1		

3.2. Experimentally measured energy consumption of the extruder main consumers

Several experimental trials were carried out to measure the energy consumption of the extruder main consumers under different screw speeds and for two different extrusion lines. The recorded energy consumption data for the drive motor (DM), barrel heaters (BH), die heaters (DH) and melt pump (MP) are shown in Table 2. Auxiliary units like circulating and vacuum pumps were excluded from energy monitoring.

Table 2
Total energy & specific energy consumption for different trials

	P1 (Type SGBE 9)		**P2 (Type SGBE 5)**	
	$\dot{m}$=176,5 kg/h	$\dot{m}$=201,7 kg/h	$\dot{m}$=80,0 kg/h	$\dot{m}$=112,7 kg/h
	v_{HO}=0,7 m/min	v_{HO}=0,8 m/min	v_{HO}=0,71 m/min	v_{HO}=1,0 m/min
	v_{Screw}=65 rpm	v_{Screw}= 70 rpm	v_{Screw}=95 rpm	v_{Screw}=128 rpm
DM	43,5 kW	47,8 kW	18,9 kW	23,0 kW
BH	0,9 kW	4,7 kW	0,5 kW	1,2 kW
DH	2,8 kW	3,8 kW	1,4 kW	1,7 kW
MP	2,3 kW	3,6 kW	1,4 kW	1,6 kW
Total E-Cons.	49,5 kW	59,9 kW	26,7 kW	27,5 kW
Specific E-Cons.	0,28 kWh/kg	0,30 kWh/kg	0,27 kWh/kg	0,24 kWh/kg

As expected, the drive motor required the most electrical energy of the main consumers for both extrusion lines. For all four trials the energy consumption of the drive motor was between 80 and 88% of the total amount. The energy consumption of all monitored elements increased with the screw speed. Conversely, specific energy consumption of extruder type SGBE 5 reduced with increasing screw speed. Previous work by Brown [6], Kelly [7], Cantor [8] and Abeykoon [9] used the same extruder type with different screw geometry and input material. Nevertheless, their results showed that the specific energy consumption increased with the screw speed. Opposing to the literature the specific energy consumption of extruder type SGBE 9 increased with increasing screw speed which is caused by a major energy consumption of the barrel heaters. This may be related to a temperature control problem during the extrusion at these parameter settings. To confirm those assumptions further tests should be performed for extruder type SGBE 9 when the installation of the control unit has been finished.

4. Concluding summary and future work

The amount of occurring waste heat out of a medium-sized extrusion line qualifies for further utilization. This is based on real-time waste heat monitoring of the vacuum chamber for extrusion line SGBE 9. The vacuum chamber waste heat monitoring shows that in chamber 1 needed most power was taken by the water to cool down the material. The higher the material output the more waste heat has been monitored. The energy consumption monitoring shows that the extruder drive consumes the most energy. Obviously a higher material output and therefor a higher screw speed leads to a higher energy consumption whereas the specific energy consumption decreases at least for extruder type SGBE 5. The discharged waste heat via barrel cooling fans will be the object of further studies. Furthermore, possibilities to use the waste heat shall be pointed out and the so for involved technologies should be developed.

4. Acknowledgements

The research activities were funded by the Government of the Federal Free State of Bavaria, (Staatsministerien für Wirtschaft und Medien, Energie und Technologie sowie für Bildung und Kultus, Wissenschaft und Kunst) with the research program “Green Factory Bavaria”. Also the companies *Hans Weber Maschinenfabrik GmbH* and *H.N. Zapf GmbH & Co. KG* supported these research activities.

References

[1] Strauch T, Gliese F, Menges G. Energy usage and conservation in extrusion plants. In: Proceedings of polymer extrusion III, London, England; 1985. p. 2-1–2-10.
[2] Drury B. The control techniques drives and controls handbook. London-UK: The Institution of Electrical Engineers; 2010. p. 308–312.
[3] Bastian M, Stübs O, Gehring A, Energie endlos sparen. Kunststoffe; 10/2009. p. 160-167.
[4] Heur RV, Verheijen M. Power quality & utilization guide: Plastics industry-energy efficiency. <http://www.leonardo-energy.org/files/root/pdf/Application/Guide/Plastics.pdf> [Last viewed 15.08.12].
[5] Barlow S. Reducing electrical energy costs for extrusion processes. SPE ANTEC technical papers; 2009. p. 1157–62.
[6] Brown EC, Kelly AL, Coates PD. Melt temperature homogeneity in single screw extrusion: effect of material type and screw geometry. SPE ANTEC technical papers; 2004. p. 183–187.
[7] Kelly AL, Brown EC, Coates PD. The effect of screw geometry on melt temperature profile in single screw extrusion. Polym Eng Sci 2006;46(12):1706–14.
[8] Cantor KM. Analyzing extruder energy consumption. SPE ANTEC technical papers 2; 2010. p. 1300–1306.
[9] Abeykoon C, Kelly Adrian L, Brown Elaine C, Vera-Sorroche J, Coates Phil D, Harkin-Jones E, Howell Ken B, Deng J, Li K, Price M. Investigation of the process energy demand in polymer extrusion: A brief review and an experimental study. Applied Energy 136; 2014. p.726-737.

3D Printing of industrial materials

Brando Okolo
INDMATEC GmbH, Kaiserstr. 164, Karlsruhe 76133
brando.okolo@indmatec.com

Abstract

There are 7 major lines of the 3D printing technology. These lines make it possible to process materials in the liquid state or solid state. Within the past 10 years there has been a drive to focus more on materials used for the production of applications-based products rather than for sampling and model/prototype development. Metals remain the most widely used industrial material. Their processing using 3D printing technologies is a challenging activity mainly because the material properties sought in printed parts are not easily realizable. The processing of composite materials using 3D printing technologies also presents some attendant problems. For instance in the case of fiber reinforced polymeric materials severe degradation of fused filament fabrication (FFF) machine parts due to abrasive wear occur. Also quality issues have been encountered with the feedstock (filament material) used in FFF modeling 3D printing technology due to poor/weak adhesion between the matrix phase and the reinforcement phase or certain desirable critical properties such as electrical conductivity are not realized. Also the printing time remains a major constraint for 3D printing of industrial materials. These factors have a direct influence on the viability of 3D printing industrial materials. Other themes covered in this short report are: (i) some process – structure - properties relationships of 3D printed parts will be discussed (ii) standardization in the 3D printing sector (iii) Business attitudes towards the 3DP technologies.

Introduction

In the field of additive manufacturing, 3D Printing (3DP) brings along a unique toolset empowering manufacturers in an unprecedented manner. The business of manufacturing using 3DP tools now cuts across different industrial sectors. 3DP tools are today used for prototyping and for the production of deployable parts. It is a technology supported in 2014 by a $4billion global market projected to grow at a compounded annual growth rate of about 46% in the period 2013 till 2018 [1]. A *Markets and Markets* forecast [2] shows that the size of the 3DP materials market will be about $408million by 2018. The introduction of new materials to the 3DP platform is a major driving force for the wider industrial application of the technology. Many industries now consider the benefits of mass customization against mass production. They are concerned about waste generation, customer-specific parts, social cooperate responsibilities and the freedom to fabricate complex part designs in a straight forward way using 3DP methods. In the midst of these concerns still lies the challenge of 3D printing industrial materials. Industrial materials fall into any of the different classes of materials: metals, ceramics, polymers, natural materials or composite materials. Some of the processes (such as melting, curing, sintering etc) inherent to the different 3DP methods define the class of material that be processed by a particular 3DP method (Table 1).

Table 1. List of different 3DP methods, material type and key printing parameters

3DP Type	Material state	Key printing parameters
- Selective Laser Melting (SLM) - Selective Laser Sintering (SLS)	- Powder; metals - Powder; ceramics, metal, thermoplastics	- Laser power - Scanning speed - Layer thickness - Powder particle size - Chamber temperature - Atmospheric gas (vacuum etc)
Electron Beam Melting (EBM)	Powder; metal	- Laser power - Scanning speed - Layer thickness - Powder particle size - Chamber temperature - Atmospheric gas (vacuum etc)
Stereolithography (SLA)	Liquid; photopolymers	- Laser power - Scanning speed - Layer thickness
Direct Light Processing (DLP)	Liquid; photopolymers	- Laser power - Scanning speed - Layer thickness
Laminated Object Manufacturing (LOM)	Solid thin sheet; paper, polymers, metals	- Laser power - Scanning speed - Film thickness
Fused Filament Fabrication (FFF) or Fused Deposition Modeling	Solid filament; thermoplastics, reinforced (particle, fibers) polymer matrix	- Printing speed - Nozzle temperature - Heat bed temperature - Chamber temperature
InkJet/MultiJet system	Powder and liquid adhesive; ceramics	- Volume of adhesive ejected - Scanning speed - Layer thickness - Powder particle size - Chamber temperature

There are 3 key aspects of the 3DP process namely (i) generation of the digital form of the part to be printed. This is usually done by computer aided design software tools or by image acquisition tools (scanners or digital camera) in 3D or 2D format, (ii) The design format is converted to an *STL format allowing for the design to be described in vector form via so-called triangulation process. The design in *STL format is sliced into 2D layers and saved in a machine readable form; G-code. The G-code represents the plan for the print-job or defines the tool-path together with the variations in printing parameters (temperature, printing speed, amount of material deposited) scheduled by the operator. (iii) The printing process in which the printed 3D object is organized from the feedstock via a layering routine. The printed 3D object may undergo a post treatment (heat, mechanical or chemical) to meet critical design requirements.

3D printed industrial materials:- influence of some processing parameters

A range of printing parameters influence the quality of 3D printed parts. Some of these have been listed in Table 1 in accordance to the kind of 3DP technology. Understanding how these parameters influence
the properties of printed parts is an important area of research for industry and academic groups. Some literature sources report on valuable correlations between properties of printed parts and printing parameters. For instance in [3, 4] results show for SLM processed stainless steel parts that as scanning speed increases the density of parts processed from powdered feedstock decreases (Figure 1).

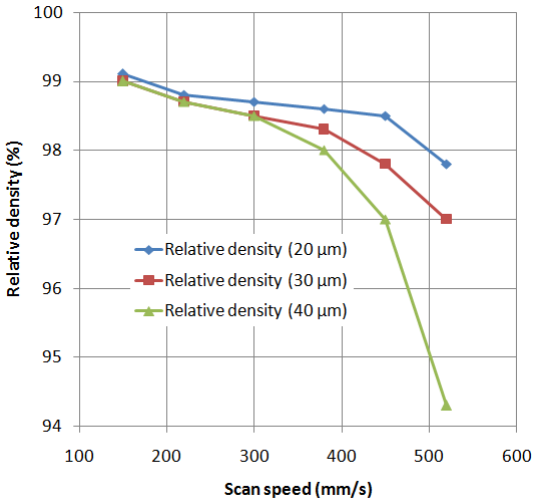

(a)

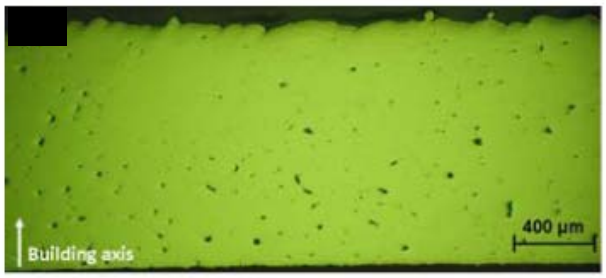

(b)

Figure 1. (a) Plot of relative density versus laser scanning speed for different stainless steel (AISI 316L) powder thicknesses, (b) Optical light microscopy image of an SLM processed AISI 316L [3]

Residual porosity in SLM 3D printed parts leads to premature component failure under relatively low mechanical loading conditions. Each pore behaves like a fracture surface thus when loaded the stress concentration that builds-up in the material results in unexpected failures. To mitigate this problem a re-melting process is introduced in the printing routine. This process involves running a second scan of the laser over freshly formed surfaces before a new powder layer is introduced for melting. Figure 2 shows the effect of re-melting on pore content in AISI 316L stainless steel.

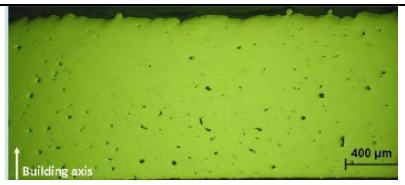

(a)

(b)

Figure 2. Optical light microscopy image of an SLM processed AISI 316L (a) before re-melting; porosity= 0.77%, density= 99.23% (b) after re-melting; porosity= 0.036%, density= 99.96% [3]. Same scale bars.

Irrespective of the kind of material being processed by the laser methods for powder bed based 3DP the trends shown in Figures 1 and 2 are typical. Also mechanical properties of SLM processed metallic parts are known to show

superior states [5] than for conventionally processed metals. Example is shown in Table 2 for the alloy Ti6Al4V

Table 2. List of comparison of the mechanical properties for differently processed Ti alloy

	E (GPa)	$\sigma_{y\,(MPa)}$	UTS (MPa)	ε_{frac} (%)
SLM (Ti6Al4V)	105 - 120	1000 - 1100	1100 - 1200	>8
ASTM (F1472 - Wrought)		860	930	>10
ASTM (F1108 - Cast)		758	860	>8

For the 3D printing of industrial materials, also printing orientation needs to be considered. Figure 3 shows the effect of printing orientation on the mechanical strength of 3D printed parts (tensile test geometry; dog-bone) [adapted from Ref. 6]. Clearly the printing strategy should be such that the part is oriented so that the principal in-plane forces act not along the loading direction when the part is in use.

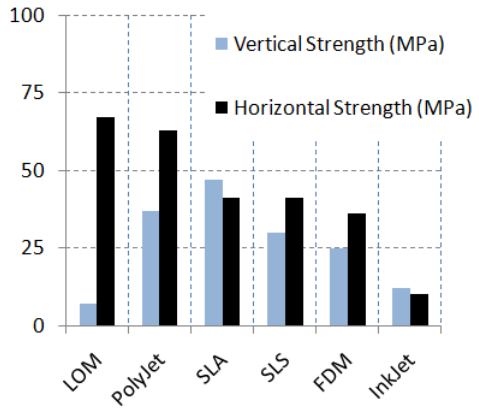

Figure 3. The effect of printing orientation on the mechanical strength of tensile test parts 3D printed using different 3DP methods [adapted from Ref. 6].

Weight reduction as a strategy for energy economy is a policy pursued extensively in the production sectors. One way this strategy is applied is by using low-weight high-strength composite materials, such as fiber reinforced polymeric materials, to replace traditional materials like metals. Only the FFF 3DP method is capable of processing fiber reinforced polymeric materials. Some machine parts of commercially available FFF machines degrade severely by processing FRP's. Figure 4 shows the impact of processing carbon fiber reinforced ABS using a printer nozzle made from brass.

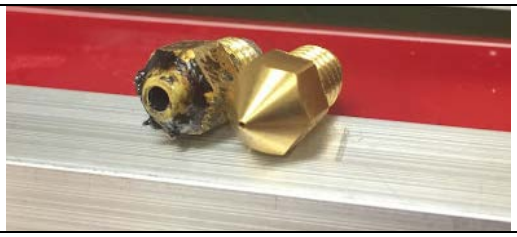

Figure 4. FFF machine brass nozzle showing material abrasive wear after printing of 750 g of carbon fiber reinforced ABS. Starting nozzle size was 1 mm.

The time needed to print industrially acceptable part is still an issue being addressed within the 3DP sector. There have however been some recent gains in this respect where printing time of parts to industry specification have been achieved in record time (see Figure 5). Continuous liquid interface production (CLIP) is a new photopolymer based 3DP system capable of fabricating parts at time 25 to 100 times less than other 3DP methods [7].

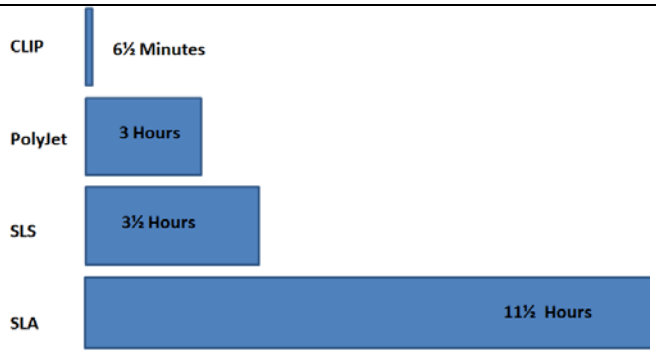

Figure 5. Comparison of time completely print given part by different 3DP methods [8].

Printing for safety and business interest in 3DP

The 3DP of industrial materials invokes questions regarding standards, certifications and verifications. In industries where safety critical parts are used, 3DP as a manufacturing tool raises concerns and anxieties. Whilst regulatory bodies such as ASTM are working develop terms for best practice in the 3DP sector agreements are yet to be reached on guidelines and standards. At the moment industries rely on rigorous testing and examination to generate the data that can offer them the confidence to deploy 3DP fabricated parts for any application. In the medical sector 3D printed parts are used for long-term implants. Sensors, control systems and engine parts fabricated from 3DP methods are now used in the automotive, aviation and in various high performance engineering applications.

These applications give credibility to the 3DP process creating new platforms on which business operations can be defined. More businesses are embracing 3DP as a solution route to a range of challenges encountered in product development, manufacturing, logistics and warehousing.

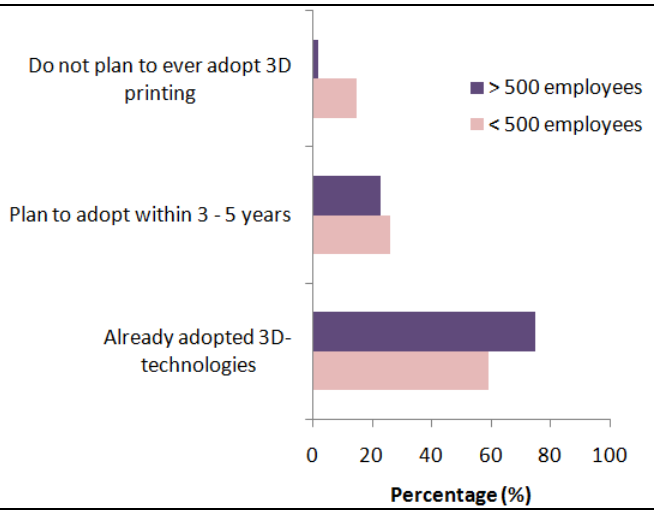

Figure 6. Comparison of attitudes towards 3DP across small and large size manufacturing business [Adapted from Ref. 9].

Reference

[1] Canalys - Report 2014/034; 3D printing market to grow to US$16.2 billion in 2018; March 2014

[2]Markets-and-Market Report: 3D printing materials market; November 2014.

[3] J.-P. Kruth ; Survey of progress in Additive Manufacturing The Leuven experience 1990-2013 From polymers to metals and beyond ; 3D Printing Event 2013 – Eindhoven.

[4] E. Yasa, T. Craeghs, M. Badrossamay, J.-P. Kruth; Rapid Manufacturing Research at the Catholic University of Leuven; US-TURKEY Workshop on Rapid Technologies; RapidTech 2009.

[5] J.-P. Kruth, G. Levy, F. Klocke, T.H.C. Childs; Consolidation phenomena in laser and powder-bed based layered manufacturing, CIRP Annals - Manufacturing Technology, Vol. 56, No. 2, 2007, p. 730-759.

[6] K. V. Wong, A. Hernandez; A review of additive manufacturing, International Scholarly Research Network - ISRN Mechanical Engineering Volume 2012; doi:10.5402/2012/208760.

1 [7] J. R. Tumbleston, D. Shirvanyants, N. Ermoshkin, R. Janusziewicz, A. R. Johnson, David Kelly, Kai Chen, Robert Pinschmidt, Jason P. Rolland, Alexander Ermoshkin, Edward T. Samulski, Joseph M. DeSimone; Continuous liquid interface production of 3D objects; Science; 20 March 2015: Vol. 347 no. 6228

2 pp. 1349-1352; DOI: 10.1126/science.aaa2397

[8] Adapted from http://carbon3d.com/

[9] PriceWaterhousewCoopers and Zpryme survey and analysis, “2014 Disruptive Manufacturing Innovations Survey,” February 2014.

Ceramic Fibers – From Roving to Woven Fabric

Sabine Olbrich, Alexandra Luft, Frank Ficker
Institute for Materials Science of the Hof University of Applied Sciences
sabine.olbrich@hof-university.de

Keywords: ceramic fiber, oxide ceramic fiber, non-oxide ceramic fiber, weaving ceramic fibers, rapier, healds, Fraunhofer, TFK, testing ceramic fibers, Nextel, CeraFib, Tyranno

Abstract

Currently, the one of the major research topics at the Fraunhofer Application Center for Textile Fiber Ceramics (TFK) is the technology of producing woven fabrics out of ceramic fibers. Due to the differences in processing behavior and specific issues to be observed, the long known procedures for standard fibers cannot simply be transferred.
In practical terms, several adjustments have to be made at the weaving machine to be able to switch from weaving standard fibers to weaving ceramic fibers. The main challenges are the gentle guidance of the yarn along whole run of thread and the twistless weft insertion. For both issues the Fraunhofer TFK already carried out tests with positive results and will soon be able to implement the plans.

Fraunhofer Institutes and Research Establishments

The Fraunhofer-Gesellschaft consists of over 60 institutes and more than 80 research institutions in Germany. It is the leading organization for applied research in Europe. The number of employees exceeds 18 000, most of them are educated in sciences or engineering. Furthermore, Fraunhofer-Gesellschaft collaborates internationally through representative offices in Europe, the US, Asia and the Middle East.

Fraunhofer Center for Textile Fiber Ceramics (TFK)

The Fraunhofer Application Center for Textile Fiber Ceramics (TFK) was found in June 2014 and is located in Münchberg. It is a cooperation between the Fraunhofer Center for High Temperature Materials and Design (HTL) in Bayreuth and Hof University of Applied Sciences. The Fraunhofer HTL belongs to the Fraunhofer Institute for Silicate Research (ISC) in Würzburg.
The Fraunhofer TFK does research on ceramic rovings and fibers. This also includes testing fiber properties like the linear density and diameter.
Furthermore, the Fraunhofer TFK examines various processing technologies by means of applicability. The laboratories and machine park of Hof University are available for disposal. The recent main focus is on weaving. Also research on the technologies of knitting, nonwoven and braiding as well as non-crimp fabrics will be carried out. Attempts in the field of nonwoven will take place as soon as the new laboratory is build up. Tests on the variation braider will take place earlier due to the fact that the machine is on-site as of late.
The third focal point at Fraunhofer TFK is to transfer the established technologies to create 2D and 3D structures out of ceramic and carbon fibers.

Ceramic fibers

Textile fibers in general are categorized by several branched properties, as shown in Figure 1. Ceramic fibers are man-made, inorganic and non-metallic. They are characterized by their high resistance against high temperatures, fire and chemical products. Further appreciable advantages are the high tensile strength of ceramic fibers as well as the applicability in lightweight constructions.

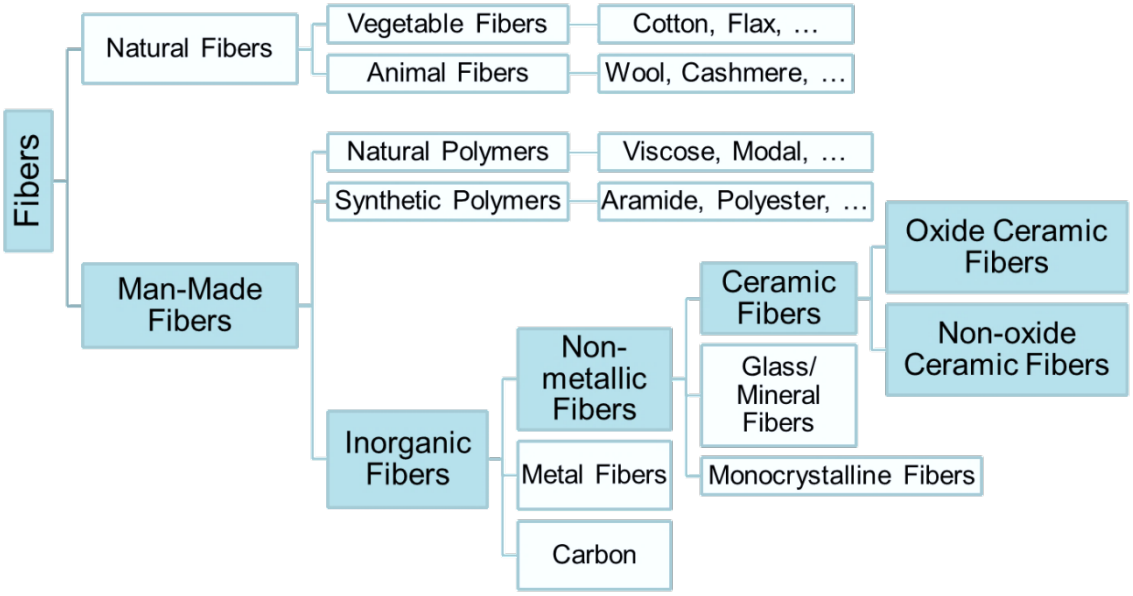

Figure 5 Classification of Fiber Types

Figure 1 also shows that ceramic fibers are subdivided into oxide and non-oxide ceramic fibers. The production stages are similar to each other. The textile pulp consists of a suspension or solution at oxide fibers and of a molten mass at non-oxide ceramic fibers. In either way it passes a nozzle and gets dried by air. Afterwards the fibers receive a heat treatment in a furnace. The last steps for both material variants are winding the fibers on bobbins as preparation for further processes.
The already mentioned characteristics like the high resistances are complemented by the properties listed in Table 1. It gives an exemplary impression about the range of variations and characteristics of different ceramic roving types.

Table 2 Comparison of oxide and non-oxide ceramic rovings (1) (2) (3) (4)

	Oxide Ceramic Roving	**Non-oxide Ceramic Roving**
Type	Alumina Fiber (Al_2O_3, Al_2O_3/SiO_2)	Silicon Carbide Fibers (SiC)
Trade names (examples)	Nextel™ (by 3M) CeraFib (by CeraFib)	Tyranno (by UBE)
Electrical conductivity	low conductivity	semi-conductive
Tensile strength	1700 - 3100 MPa	1600 - 4000 MPa
Modulus	150 - 380 GPa	170 - 420 GPa
Price	260 - 790 €/kg	1000 - 8500 €/kg
Optical appearance	white	black
Linear density	67 - 2550 tex	180 - 200 tex
Diameter of the single filament	7 - 20 µm	7 - 14 µm
No. of filaments	400 - 900	800 - 1600

The selection of the fiber type is made by the individually required properties. The most values of non-oxide ceramic fibers are higher compared to oxide ceramic fibers. On the other hand non-oxide ceramic fibers are high-priced.
Intended applications for ceramic fibers are those, where high temperature resistance and high strength are required at the same time. The temperature resistance thereby can also provide functions like insulation, flame barriers and thermal protection.
The fields of application are protective clothing, aero- and outerspace technology, automotive industry, kilns and furnaces.

Performed Tests at Fraunhofer Center for Textile Fiber Ceramics (excerpt)

The Fraunhofer TFK tests fiber and yarn properties like the number of filaments within a roving, the tensile strength of single fibers and rovings as well as the minimal bending radii.
To improve the processability and to “glue” the filaments together, sizing is applied to multifilaments of ceramic fibers. For testing the properties of single fibers the sizing agent has to be removed. This is either carried out thermally or by solvent, both techniques are available at Fraunhofer TFK. For both cases the principle of the underlying procedure is identical. The prepared sample is weighed out at first. The second step is to remove the sizing, either thermally in a muffle furnace or by solvent in a soxhlet extractor. After weighing the desized sample the size content is calculated.
A further performed test at Fraunhofer TFK is the determination of the tensile strength of filaments as well as of multifilament tows. For testing single filaments desizing has to be carried out first. In either case the test item is glued in paper frames to increase the stability and to prevent from breaking while fixing the sample in the clamps of the machines. After carrying out the tensile test the tensile strength of the fiber is calculated by the tractive force and the cross-sectional area of the test item.

Weaving ceramic fibers

Weaving is one of the oldest fabric forming technologies, yet the application for ceramic fibers represents a challenge.
The general principle of weaving is shown in Figure 2, where the production direction is from left to right. The warp yarns are stored on the beam. On the run of thread they pass the healds, which are responsible for shedding. A vertical movement raises and lowers the shafts with the healds to create the shed for inserting the weft yarn. This insertion process is also called “picking”.
As soon as the weft yarn passed the machine in cross direction, the reed pushes it to the fell of the already woven part of cloth. This operation is called “beating up”. The last step during the weaving process is winding the woven fabric on the cloth beam.

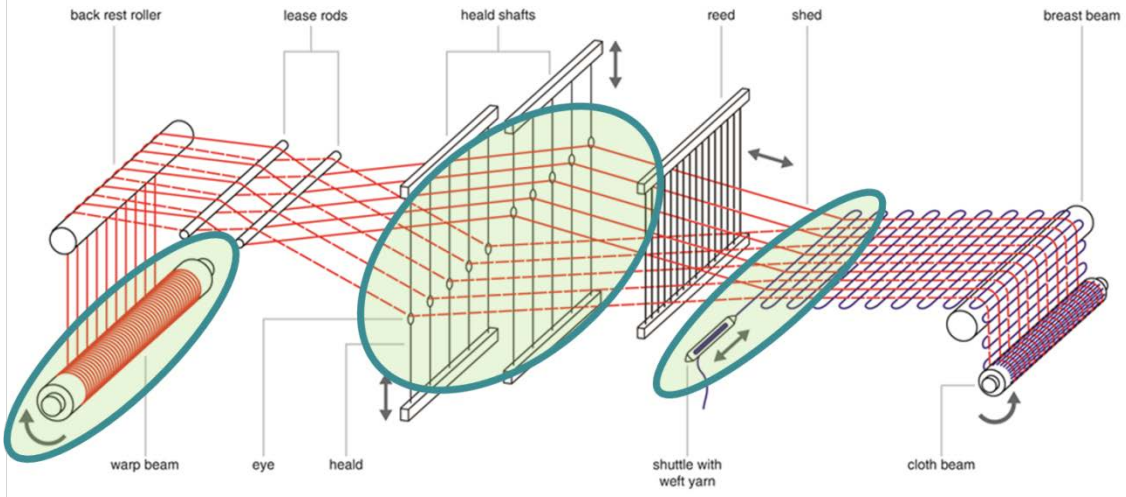

Figure 6 Principle of weaving

In general, the brittleness and breaking tendency in case of loads in cross direction results in several guidelines for the practical feasibility of weaving ceramic fibers. Knots have to be completely replaced by other joining techniques like glueing. In general sharp edges and small radii have to be avoided to prevent the roving from breaking.
Additionally, figure 2 points out the elements of a weaving machine, which are challenging when it comes to weaving with ceramic fibers, namely the warp feeding system, the healds and the weft insertion system as well as the assurance of a twistless weft insertion.

Warp feeding system
The first one is the warp feeding system. Standard weaving machines are equipped with beams, where all warp yarns are stored. The alternative is a creel, which increases the flexibility and handles the rovings more gently. The disadvantages of creels are the investment costs for procuring and the large space requirement.

Healds
Standardly twin or flat steel wire healds are utilized. To increase the gentle treatment of the processed yarn different heald types may be applied. One possible design that is shown in Figure 3 consists of two cylinders forming the heald eye. The larger and obtuse contact angle is carefully guiding flat tape yarns.

The second presented special heald is made of polyester and is applicable at handlooms only. Like the heald with two cylinders it guides the yarn without twisting it due to flat contact areas.

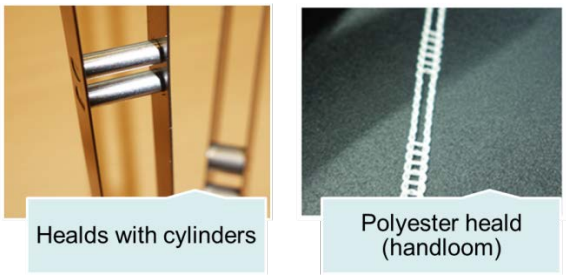

Figure 7 Healds for special applications

Weft tension
The weft tension is commonly generated by a filling feeder. This device adds some twists per length unit due to its construction.
For inserting ceramic weft yarns an alternative is necessary to keep it twistless. The apparently best solution is to store the yarn a loop-shaped form.

Weft insertion system
Historically, there are several weft insertion system. The shuttle system poses the advantage of solid selvedges, but permits only a small pirn with weft yarn to be stored inside the moving shuttle.
Besides, weft yarns are picked by projectiles, jets or rapiers, all with the advantages of more weft yarn storage, smaller required sheds and higher productivity. At projectile insertion systems, the weft yarn is clamped in a projectile and shot through the shed. Jet systems like the air jet system transport the weft yarn through the machine via an air flow.
Additionally to those benefits, the insertion by rapiers carefully clamps the ceramic rovings. Tests already confirmed the possibility of picking ceramic rovings with the help of rapiers.

Bibliography

1. **Cherif, Chokri, [Hrsg.].** *Textile Werkstoffe für den Leichtbau.* s.l. : Springer-Verlag Berlin Heidelberg, 2001. ISBN 978-3-642-17991-4.

2. **3M.** NextelTM - Ceramic Textiles Technical Notebook. [Online] [Zitat vom: 01. June 2015.] http://www.3m.com/market/industrial/ceramics/pdfs/Nextel_Tech_Notebook_11.04.pdf.

3. **UBE America.** Tyranno. [Online] [Zitat vom: 01. June 2015.] http://northamerica.ube.com/content.php?pageid=54.

4. **Eichhorn, Stephen.** *Handbook of Textile Fibre Structure.* s.l. : Woodhead Publishing, 2009. ISBN 9781845693800.

Conductivity of printed electronics

Annette Wimmer, Herbert Reichel
Institut für Materialwissenschaften der Hochschule Hof
annette.wimmer@hof-university.de, herbert.reichel@hof-university.de

Keywords: printed electronics, conductivity, high pressure forming, back-molding

Abstract

Back-molding of polymer films is a sub-procedure of manufacturing MIDs. Integration of capacitive electronics in three dimensional molded devices offers many advantages for automotive, medical and other applications. Currently, almost flat production is possible. To realize 3D-components, an adapted forming process and further material investigations are necessary. The most important evaluation criterion for the production process is the remaining electrical conductivity of the final product. This paper summarizes the results of initial investigations on formed film samples. Different conductive adhesives and polymer films were used. Conductive structures were obtained by screen printing and electrolytic deposition.

Introduction

In-mold-labeling is an established technology to realize three-dimensional, decorated, resistant structural components. Additionally, the production of two-dimensional printed circuit boards (PCBs) are state of the art. A particular challenge is the integration of electronics in three-dimensional carrier systems under specific aspects. The aim of the investigation is to combine design and electronics via a compact multilayer-hybrid system, consisting of a design- and a functional layer, combined in a molding process.
Three-dimensional user-interfaces with printed electronics enable easy operation without additional keys.
Hence, the installation of mechanical operating knobs, switches and buttons becomes unnecessary. The clear arrangement of the operation panel with high decorative freedom allows a space-saving integration of the components with small dimensions. The properties mentioned above create new opportunities for applications. Currently, integrated electrical applications are consisting of complex, cost-intensive rigid-flex printed circuit boards that can be divided in different sections. The first layer is a non-conductive protective layer, primarily consisting of polymers, to save electronics and design. The second layer is a functional layer, a structured polymer film, working as a sensor using capacitive fields. Additionally, the third layer is a providing layer that contents of the control electronics and organizes data flows.
Nevertheless, the construction of these multilayer set-ups requires a huge amount of installation work and costs. To date, it has not been possible to realize real three-dimensional assemblies. There is an urgent need for techniques, which can reduce the necessary effort and to make more spatial components possible.
Therefore, an election of suitable material is needed, the three-dimensional formable polymer films for the design- and functional layer, injection-molded circuit carriers, rigid-flex-PCBs and IML components. As part of the “foltronic”

research project, the institute for material science at Hof University performed a series of measurements. The focus remained on the evaluation of electrical conductivity of printed conductor lines on polymer films at different grades of elongation. The stretching was achieved by tension-tests on the one hand and by high-pressure-forming processes (HPF) on the other hand. The impact was analyzed by conductivity-tests, evaluation of adhesion-tests and microscopic investigations. Additionally, different thermal analyses are necessary, to see, if the conductor-lines pass the power load with different currents.

Basics of printed electronics

There is a high potential to efficient manufacturing of space-saving electronics with printing conductor lines on very flat and light weight polymer films. The therefore used processes have the origin in the graphical printing industry, however the processes have to be adapted or modified for printing electronic structures. Different printing methods can create electrical devices on different substrate materials. Most important criterion for the selection of the used printing technology is throughput and precision. The technologies can be roughly split up into screen based and roll-to-roll based materials. With screen based processes, high precision is achievable by a lower volume of throughput. These processes are particularly suitable for applications at a laboratory scale for the purposes of research. The roll-to-roll processes are used for a high volume production.
Printing of electronics has different advantages. Optimally, no time-demanding intermediate stages in production-processes are needed. Masking processes, separation and reworks become redundant.
The application of functional layers on flexible substrates allows mechanical flexibility and a high degree of form freedom of the final product. Widespread electronics can be produced and it is possible to realize low cost and efficient production.
Depending on the process, inks and pastes can be applied on substrate surfaces to produce conductors, semi-conductors, insulators or electroluminescent or photovoltaic materials.
The most frequently used polymer materials are PC, PET, PEN, PVC, PC/ABS, PC/PBT, PMMA, PMMA/PVDF, ABS, PB, and PEI, but also ceramic materials are possible. Likewise, the variety of the printing materials is also comparatively large. Organic pastes or liquids, metal based materials can be applied almost in the same way as nano particle based materials.

Foltronic project

The idea of the foltronic project is to combine the design or protective layer with the functional layer to the hybrid. The functional layer consists of capacitive touch pads. Printing on polymer films is an essential process in development of 3D- design components. The samples for the foltronic- project were printed in a screen printing process and the copper pastes systems by an electrolytic deposition process. The design consists of several conductor lines in different line widths and other usual conductive forms. In the second step, a high pressure forming process is performed on the film (Fig. 1). The formed three-dimensional components are back-molded with a thermoplastic polymer. As seen in in Fig. 2.

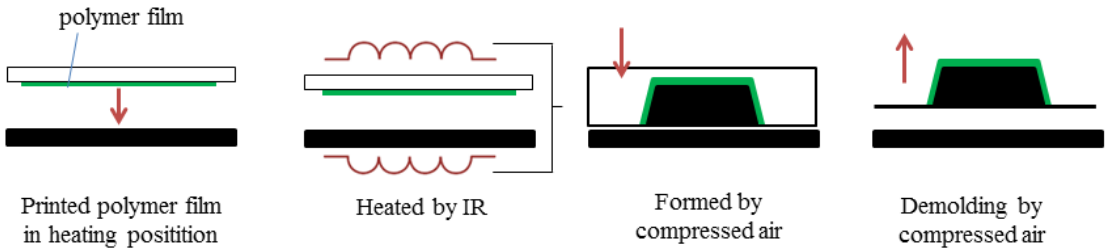

Fig. 1: High pressure forming process

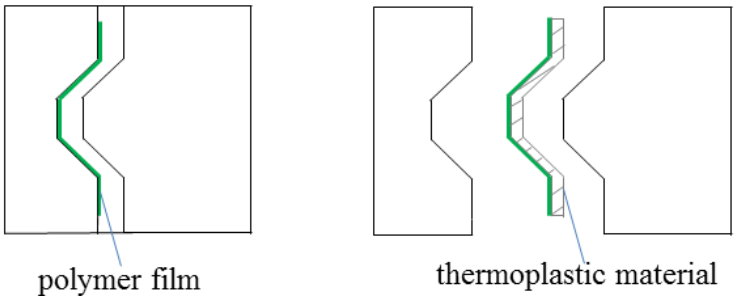

Fig 2: Back Molding of printed structures

Due to the deformation during the forming process, electrical conductivity is affected. The proportions were tested in different tests. Seven different combinations of material were tested for the investigations. Table 1 shows the relevant materials that were selected based on essential requirements of automotive suppliers.

Table 1: Materials used for investigations

sample		**Substrate**		**coating**	
Nr.	**Type**	**Material**	**Film thickness**	**Material**	**Layer thickness *d***
1-1	Pedot: PSS	PC	250 µm	PEDOT : PSS	4 µm
1-2	Ag1	PC	250 µm	Ag	4 µm
1-3	Ag2	PC	250 µm	Ag	17 µm
1-4	Ag3	PC	250 µm	Ag	7 µm
3-5	PEPE	PET	125 µm	PEDOT	17 µm
4-6	Cu1	PET	125 µm	Cu	18 µm
5-7	Cu2	PET	50 µm	Cu	5 µm

Surface resistivity before and after tension test

As a base of the investigations, the surface resistivity was measured with a 4-point measurement system. Four needles were positioned in the middle of the parallel printed conductor lines with a line width of 1mm to determine the surface resistivity. With the measured layer thickness of the paste, the calculation of the specific electrical conductivity is possible via multiplication. The conductivity is actually just the opposite aspect of the specific electric resistance. Additional investigations were done after a tension test according to DIN EN ISO 527-3/2/50 and several defined steps of mechanical force. The

influence of the elongation on the conductivity was verified. Figure 3 shows the results of the measured conductivities.
Over all samples the conductivity decreases with increasing strain. Striking reductions are visible between 5 and 10 percent of strain. Plastic deformations appear over the entire cross section of the sample. Transition from elastic to plastic deformation appears for PC at a strain of 2% and for PET at 1.5%. The substrate materials show differences in the necking. At PC necking appears at 8% and for PET at 6% of strain.
The sample with Pedot:PSS shows a small overall reduction of the conductivity. At this polymer conductor no charge transport via quantum transitions is possible, but via inter- and intramolecular hopping processes.
The intramolecular transitions occur along the orbitales (strain of main-chains). In the majority of the samples, at a strain of 20%, the conductivity collapses, the contact surface of the silver particles is no more sufficient. For the copper conductor lines a good conductivity is visible over the entire measurement range.

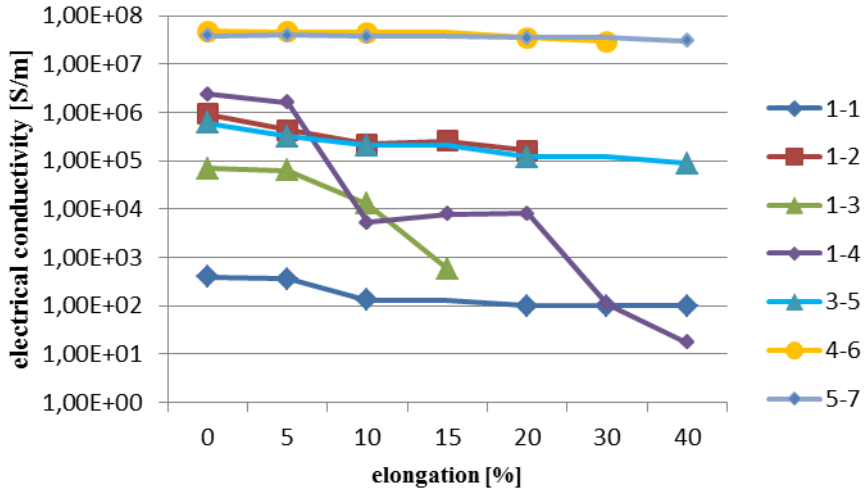

Fig. 3: conductivity at a defined elongation

Furthermore Ag/PC samples were tested according to their additional coating. Reference samples and samples with a black decor print under the conductive layer. The result was a higher conductivity of the conductor lines without decor layer.

Adhesion test

Further the printed layers were also evaluated on the basis of their layer adhesion. All material combinations were subjected to a cross cut adhesion test acc. DIN EN ISO 2409 (2 mm spacing, layer thickness 0-60µm for soft substrates) to assess adhesion properties and interactions between substrate-system and coating technology. The sufficient adhesion is the base for a reliable determination of electrical conductivity. All samples were classified into GT 0, the best class with no significant defects after removing the tape. As a result, screen-printing is a good method to apply an adhesive layer.

Microscopic analyses

In the framework of the microscopic analyses micro-cracks were detected, these may affect the conductivity. Visible damages are possibly intra-molecular in the silver particles and not through the whole coating (Fig.4). Even bridging of

micro-cracks is possible. The sample of 1-3 und 1-4 shows cracks already at an elongation of 10%. A low contrast complicates the assessment especially at the organic pastes.

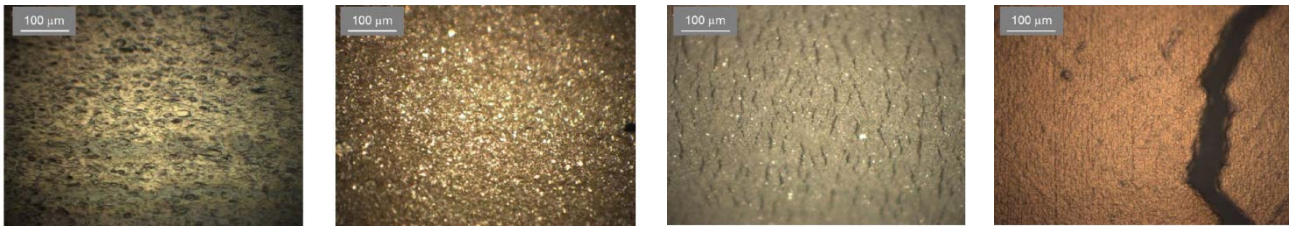

Fig 4 microscopic images magnified 500 times

(sample1-1 after 40% elongation, 1-2 after 30% elongation, 3-5 and 4-6 after 40% elongation)

Thermographic investigations

For thermographic investigations images were taken after contact with power supply at a current of 50mA and100 mA and duration of five minutes. The resistivity of the structure is 250Ω. The thermographic images were taken in 30s intervals. At the transparent sample thermal deformation of the film was visible at a current load of 100mA. The assessment of the images shows a temperature of more than 150°C, what would damage the polymer film.

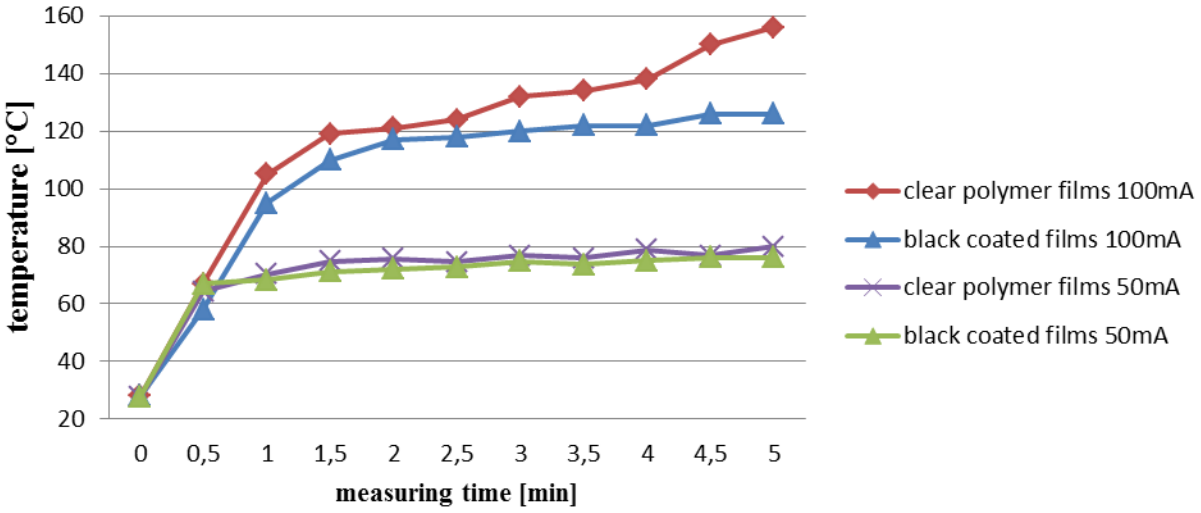

Fig 5 thermographic analyses of printed structures

Although the black samples resulting a lower initial electrical conductivity, examination of the thermal images shows a more uniform heat distribution. If the decor printing paste contains carbon, heat dissipation is more even in comparison to the clear samples. Consequently, a coating can help to avoid hot-spots on electronic devices.

Summary

The conductivity depends on the stage of elongation. Printed, conductive structures have to be adapted to the forming design, to reach and guarantee the best possible electrical conductivity. Screen-printing processes with different material combinations is feasible and can open up new opportunities for printed electronics. The adhesion test of the printed layers shows good results, if a

screen printing technology is used. Further printing technologies will be analyzed in more detailed investigations.
Additionally, different parameters in the back-molding process have to be tested, focusing the impact of temperature and pressure on the conductivity.

Acknowledgements

The investigations were funded by the Bavarian Government “Bayerischer Staatsministerium für Wirtschaft und Medien, Energie und Technologie” within the research program “Mikrosysteme Bayern”. The research project “foltronic” [MST-1203-0004//BAY171/003] included industrial partners (Midtronic, Wiesau, Germany; KH Foliotec GmbH, Sparneck, Germany) and the research institutes “FAPS” at the Friedrich-Alexander-University Erlangen-Nuremberg and “ifm” at the Hof University of applied sciences.

References

[1] Information on www.niebling.de
[2] Information on www.kunststoff-know-how.de date 03.04.2015
[3] J. Franke, 3-D MID e.V.: Three-Dimensional Molded Interconnected Devices (3D MID), Hanser-Fachbuch-Verlag, München 2014
[4] Weigelt, Karin: Integration gedruckter Elektronik in Kunststoffe durch Folienhinterspritzen, Dissertation, Technische Universität Chemnitz, 2014
[5] Information on www.hanser-automotive.de/uploads/media/FA_Atmel_stemp.pdf date 01.07.2015
[6] Information on http://elektronik.pr-gateway.de/atmel-prasentiert-konzept-einer-gebogenen-mittelkonsole-mit-touch-bedienung-zum-ersten-mal-auf-der-ces-2014/ date 01.07.2015
[7] Information on http://www.films.bayer.com/en/Technologies/Thermo-Forming-High-Pressure-Forming.aspx date 01.07.2015